Lean ignition and blow-off behaviour of butyl butyrate and ethanol blends in a gas turbine combustor

Zhichao Zhang [a,b,c], Longfei Chen [b,*], Yiji Lu [a,c,*], Anthony Paul Roskilly [a,c], Xiaoli Yu [a,c], Andrew Smallbone [a], Yaodong Wang [a]

[a] *Department of Energy Engineering, Zhejiang University, Hangzhou, 310027, China*

[b] *School of Energy and Power Engineering, Beihang University, Beijing, China*

[c] Sir Joseph Swan Centre for Energy Research, Newcastle University, Newcastle NE1 7RU, UK

HIGHLIGHTS

- Lean ignition and blow-off of butyl butyrate-based biofuels were reported;
- Butyl butyrate-based biofuels are easier to be ignited and more difficult to be blown off in a GT combustor were conducted
- Two new equations successfully predicting key combustion performance were proposed;

Abstract

This paper reports the experimental study on lean ignition (LI) and lean blow-off (LB) behaviour of butyl butyrate-based biofuels in a gas turbine combustor. The butyl butyrate-based biofuels were formulated (butyl butyrate - ethanol blends with volume percentage of ethanol 0, 10%, 30%, 50%

* Corresponding author. Tel.: +44 (0) 191 208 4827
E-mail address: chenlongfei@buaa.edu.cn (L. Chen)
yiji.lu@ncl.ac.uk; luyiji0620@gmail.com (Y. Lu)

respectively, named BE-0, BE-10, BE-30, BE-50). The aviation kerosene RP-3 was also tested as a reference fuel. A combustor of an aero-engine was fabricated to conduct experiments on these fuels. The statistic method Design of Experiments (DoE) was employed to correlate LI and LB with fuel properties and operating conditions, and then analyse the significance of these experimental variables. The results indicated that all test biofuels had lower equivalence ratio of LI than RP-3, but the LB between RP-3 and the biofuels of high ethanol fraction (30% and 50%) had no appreciable difference at low air flow rate. The results also demonstrated that fuels with high ethanol fractions tended to ignite and blow off the flame at higher equivalence ratios. Meanwhile, the equivalence ratio of both LI and LB decreased at high inlet air flow rate for all the test fuels. RP-3 could combust under a larger range of air conditions yet its stability was more sensitive to air flow rate than test biofuels. Two predictive equations of LI and LB were obtained via Design of Experiments (DoE) and demonstrated that the lower heating value (LHV) of fuels, air pressure drop in the combustor, fuel pressure and inlet air pressure of the combustor were the main factors influencing LI and LB.

Keywords: Gas turbine combustor; Butyl butyrate; Ethanol blends; Lean ignition and blow-off behaviour; Design of experiments.

Nomenclature

ANOVA	Analysis of variance
BE-x	Butyl butyrate- x% ethanol (volume)
DoE	Design of Experiments
Hr / LHV	Lower heating value
H_{vap}	Enthalpy of vaporization

LB	Lean blow-off
LI	Lean ignition
LSCR	Leanest stable combustion range
P_a	Inlet air pressure
P_f	Fuel pressure
RSM	Response Surface Method
SMD	Sauter Mean Diameter
ΔP	Air pressure drop of the combustor
$\emptyset$	Equivalence ratio
ρ_f	Density of fuels
ν_f	Kinematic viscosity of fuels
σ_f	Surface tension of fuels

1. Introduction

Gas turbine engines have played a pivotal role in advancing power generation and transportation technology over the past decades [1]. The increasing cost of aviation kerosene and ever stringent emission regulations of aircrafts issued by the International Civil Aviation Organization (ICAO) Council [2] spur the advancement of combustor technology and alternative aviation fuel usage.

The study on aviation biofuels attracts increasing attentions as alternative energy resources to petroleum-derived fuels with comparable engine performance while mitigating pollutant emissions [3]. Seljak *et al.* [4] burnt liquefied lignocellulosic biofuels in a gas turbine and found

a significant reduction of NO_x and PMs emissions compared to diesel fuel. Habib *et al.* [5] studied the performance of four types of biofuels and their blends with Jet A and revealed that biofuels could reduce the thrust-specific fuel consumption, the CO and NO_x emissions of a gas turbine engine. However, some properties of biofuels such as low energy density, high melting point and flash point, high viscosity and poor thermal stability may exert a negative impact on atomisation and combustion, and thus fail in meeting current aviation standards [6]. Jenkins *et al.* [7] and Chuck *et al*. [8] tested physical properties, energy content, oxidative stability and toxicity of several single-composition biofuels and compared with fossil fuel counterparts. Results indicated that butyl butyrate ($C_8H_{16}O_2$) has similar viscosity, flash point, distillation profile and low temperature behaviour to kerosene (Jet A) and relatively higher energy density compared to other biofuels. Therefore, researchers concluded that butyl butyrate is not only a qualified biofuel surrogate but also fully compatible with aviation kerosene. The comparison of the properties of these biofuels are shown in Figure 1 according to literature [7] and [8]. The authors [9] have recently reported the study of combustion and emissions performance burning butyl butyrate in an aero-engine combustor and found it produce significantly lower NO_x and particulate matters than kerosene.

The lean ignition and lean blow-off are important characteristics to evaluate the combustion performance of new fuels, which reflects the combustion stability. Naegeli and Dodge [10] conducted combustion experiments in a gas turbine combustor on ten different fuels at constant air flow rate and found that the viscosity of fuels, fuel temperature and fuel droplet size were the most significant factors impacting ignition at low air temperature. However, the effects of air flow rate or air velocity were not considered in their study. Jones and Tyliszczak [11]

employed Large Eddy Simulation (LES) in conjunction with the filtered probability density function (PDF) equation to explore more factors which influences ignition in a gas turbine engine and demonstrated that spark size was also an important parameter in the ignition process. Esclapez et al. [12] used the LES to study the effects of fuel properties on ignition and blow-off in a gas turbine combustor and found alternative fuels with lower cetane number could be ignited faster and had more stable lean blow-off limit. Esclapez et al. [13] tested the blow-off of several fuels via large eddy simulation (LES) approach and found the change in the recirculating gas temperature and position weaken the evaporation process and lead to a complete extinction of the flame in the primary zone of the combustor. Nevertheless, most of previous studies were conducted by simulation, yet the experimental investigations in real gas turbine combustors were rarely reported in terms of engine ignition and blow-off. In order to study the ignition and blow-off experimentally, Deng et al. [14] investigated the diffusion flames of dimethyl ether at elevated pressures in the counter flow, and found that the increasing ambient pressure and oxygen concentration promoted heat release and extended the gap between ignition and blow-off. Phuoc et al. [15] explored the impact of spark location on ignition and blow-off and found that the ignition was the easiest at two locations: the vicinity of the nozzle tip at the axis and far field from the nozzle tip at the place 4.5 mm off the axis. However, previous researches primarily investigate the ignition and blow-off of diffusion flame in burners, yet the burner conditions are not representative to those in a gas turbine combustor.

Few researchers took efforts in quantitively correlating the lean ignition and lean blow-off to experimental variables of the combustor of gas turbine engines. Lefebvre [16] gave the

equations of ignition and blow-off relevant to air conditions, fuel properties and the geometric characteristics of combustors. However, the significance of each parameter and the interaction among them were not considered. Design of Experiments (DoE) is a statistic method containing several approaches for designing experimental variables and analysing results [17]. It has been widely used in various fields and not only can reduce the amount of experiments but also correlate experimental variables to results with the analysis on the significance of each independent variable [18, 19]. However, only a few researchers in fuel spray and combustion have used DoE in their studies. Chen et al. [20] used the Mixture Design Method (MDM) of DoE to formula fuels and analyse the particles emitted from a GDI engine. Nevertheless, the MDM method is particularly for the design of compositions of mixtures but cannot adapt to designs associated with independent variables, which limits its application in more fields. Another approach named Response Surface Method (RSM) of DoE was introduced in a previous study [21], where the researchers formulated a semi-empirical model to correlate the Sauter Mean Diameter (SMD) of spray to several independent experimental variables such as fuel pressure, fuel density and air pressure. Therefore, the RSM is expected to be an effective tool for the research on combustion, which has never been considered yet. Via the RSM approach, we can correlate the lean ignition and blow-off to experimental variables in the combustor with high precision, and analyse the significance of all variables.

In summary, biofuel is a sustainable energy resource for gas turbines or aero-engines with the advantage of lower pollutant emissions. However, most biofuels have poor viscosity, distillation profile and low temperature behaviour, which have negative impacts on atomization and combustion. In addition, the research on ignition or blow-off was rarely reported and no

quantitative analysis has been done with the analysis of significance. In order to evaluate the potential of new biofuels, which have closed properties to aviation kerosene, butyl butyrate-based biofuels were employed in a gas turbine combustor to investigate their characteristics of lean ignition (LI) and lean blow-off (LB). Meanwhile, the Design of Experiments method has been adopted to reveal the quantitative relationship between the LI and LB with experimental variables and their interactions.

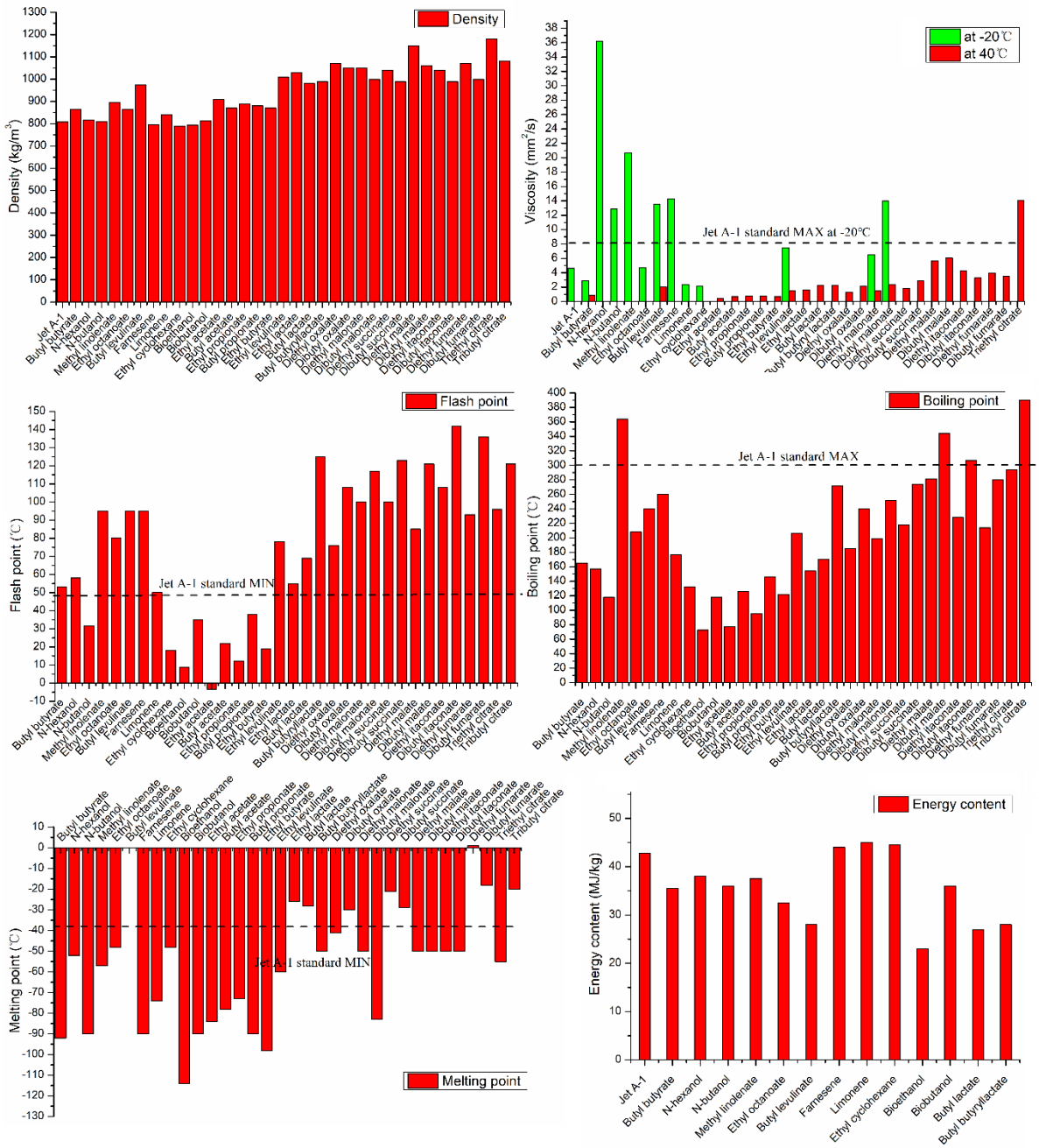

Fig. 1. The comparison of the properties of biofuels

2. *Apparatus and Methodologies*

Test fuels

Butyl butyrate was chosen to be the primary component of the test biofuels. Its main physical and chemical properties are from the NIST data base, as shown in Table 1.

Table 1
Physical and chemical properties of butyl butyrate

Property	Molecular Weight (g/mol)	Melting Point (℃)	Flash point (℃)	Boiling point (℃)	Vapour Pressure (mm Hg)
Butyl butyrate	144.214	-91.5	53	165	10.34

Although butyl butyrate has relatively higher energy density compared to other biofuels, the poor volatility and the higher surface tension of butyl butyrate may exert a negative impact on atomization and combustion. Previous literature [22-24] demonstrated that ethanol can provide a stable combustion with low emissions in gas turbines, and the mixture of butyl butyrate and ethanol would be a good candidate of aviation biofuels. In this study, ethanol was blended with butyl butyrate by volume fraction 0~50%, and lean ignition and blow-off of the test biofuel blends were investigated in a low pressure aero-engine combustion system. The aviation kerosene RP-3 was used as a reference fuel.

The main properties of four test fuels and RP-3 are listed in Table 2, where BE-0 stands for butyl butyrate, and its ethanol blends are termed as BE-10, BE-30 and BE-50 with the numbers representing the volumetric fractions of butyl butyrate. The density and viscosity of test fuels were measured by an SNB-4 stepless speed rotary Digital Viscometer and the surface tension

was measured by an YW-200A surface tension measurement device. The lower heating value (LHV) of butyl butyrate and kerosene were obtained from literature [7]. The evaporation enthalpy of butyl butyrate, kerosene and ethanol were from the NIST database. As butyl butyrate and ethanol have similar molecular polarity, the activity coefficients of them are nearly unity, which makes their blends not highly non-ideal liquid. In addition, according to Hess's Law, the evaporation enthalpy of blended fuels could be derived by measuring the enthalpy of mixing [25], which turned out to be negligible in this study. As a result, the evaporation enthalpy of the fuel blends can be approximately obtained by linear average.

Table 2

Main properties of test fuels

Fuels	Mean formula	Viscosity at 15℃ (mm^2/s)	Surface tension at 15℃ (mN/m)	Density at 15℃ (g/cm^3)	Evaporation enthalpy (kJ/mol)	Lower heating value (MJ/kg)
BE-0	$C_8H_{16}O_2$	1.194	26.41	0.8692	40.15	35.0
BE-10	$C_{6.56}H_{13.6}O_{1.76}$	1.166	24.81	0.8612	39.99	34.1
BE-30	$C_{5.43}H_{10.51}O_{1.45}$	1.157	23.84	0.8457	39.67	32.3
BE-50	$C_{3.56}H_{8.61}O_{1.26}$	1.130	22.77	0.8296	39.36	30.5
RP-3	$C_{10.35}H_{20.83}$	1.255	25.32	0.7967	50 ~ 60	42.8

Experimental apparatus

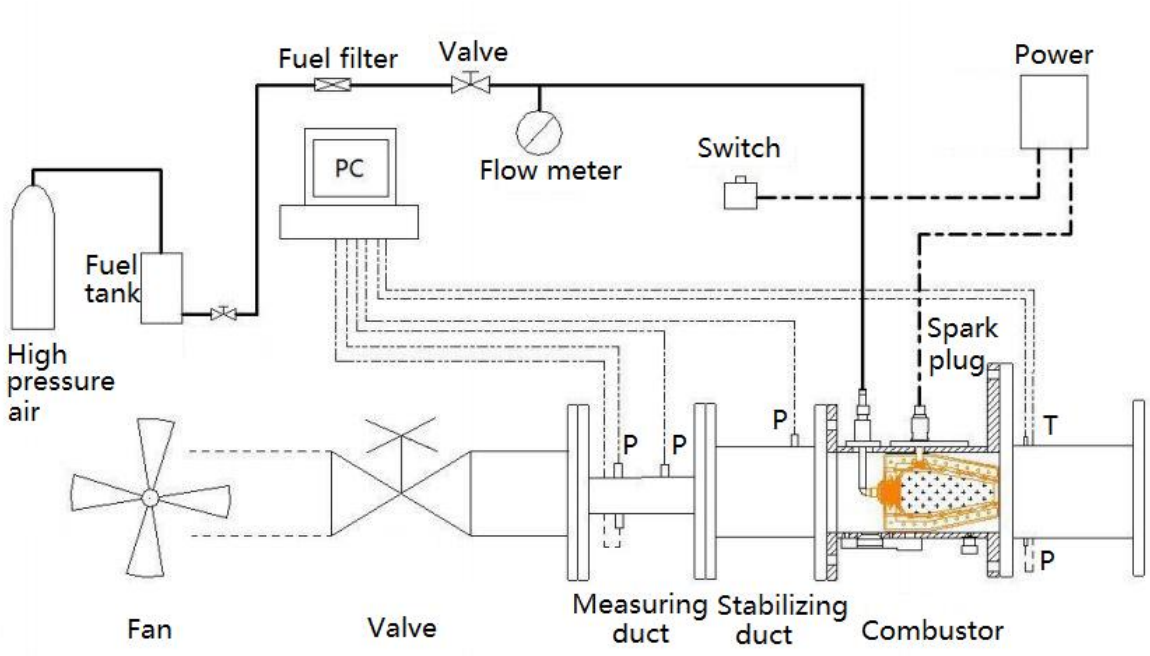

Fig. 2. Schematic diagram of the gas turbine combustor system

The experimental system was developed to conduct the experiments on ignition and blow-off, as shown in Fig. 2. The system consists of the air flow route and the fuel feed route. In the fuel feed route, the fuel in the tank is pressurized to 2MPa by high pressure air and then delivered to the air-blast nozzle in the combustor via a fuel filter, a valve and a Coriolis mass flow meter. Meanwhile, the air at room temperature is blown by a fan, through the measuring duct and stabilizing duct, and eventually to the combustor. A 12 J spark plug is installed in the combustor to produce sparks for ignition. The conditions before and after the combustor, e.g., the inlet air pressure and the outlet pressure and temperature, can be measured by the pressure transducers and K-type thermocouples in the air flow route. All the signals are monitored by a LabVIEW program via a National Instrument data acquisition card.

The combustor as shown in Fig. 3 is fabricated based on an aero-engine. As the combustor in the aero-engine is annular, only a sector of the combustor is employed to reduce fuel consumption and to enable accurate control of inlet conditions. Fuel spray is generated

by an air-blast nozzle, which consists of a centrifugal atomizer with the orifice size of 0.5 mm, a swirler and a venturi tube. The fuel is injected with the cone angle of 67° by the nozzle onto the wall of the venturi tube and thus forms liquid film, which then breaks to droplets by the air from the swirler. The swirler has double swirling components, an inner swirler and an outer swirler, whose effective areas are 112.8 mm^2 and 96.6 mm^2, and thus have the swirling number of 0.91 and 0.93 respectively. The inner swirler produces clockwise tangential flow by oblique holes, whilst the outer swirler generates anti-clockwise axial flow via axial blades. The throat of the venturi tube, which is 11.5 mm from the outer swirler, has a diameter of 17.44 mm. The entire zone in the flame tube includes the primary zone and dilution zone. The fuel-rich combustion occurs in the backflow caused by the air from the head and the primary zone holes, and then evolves to lean combustion due to dilution air. The case of the combustion chamber is 172 mm high and 325 mm long with the thickness and width of the case wall being 11 mm and 145 mm.

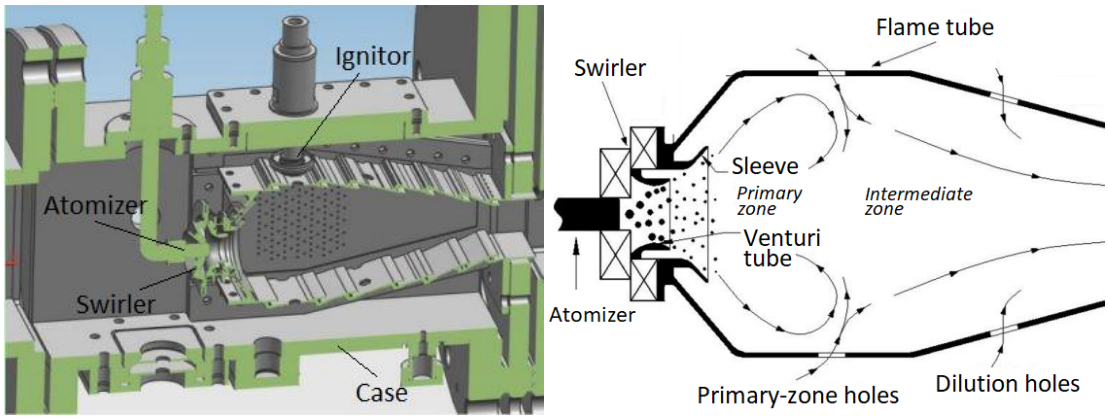

Fig. 3. Section view of the combustor chamber

Table 3 shows the residence time of the combustor at the inlet air pressure of 2 MPa and temperature 600 K. The distribution of the inlet air flow is designed and listed in Table 4, which indicates the percentage of air mass flow through each zone of the combustor.

Table 3
Residence time of the combustor

Zone	Mass flow (kg/s)	Density (kg/m^3)	Volume (mm^3)	Residence time (ms)
Entirety	1.64	11.61	1120722	7.94
Primary zone	0.70	11.61	265796	4.40
Intermediate zone	1.01	11.61	645654	7.43

Table 4
The distribution of inlet air mass flow

Zone	Primary zone holes	Dilution holes	Flame tube cooling holes	Head cooling holes	Swirler	Side wall cooling holes
Air mass (%)	14.02	17.70	32.56	14.41	17.32	3.99

Procedure of experiments

The main inlet variable of the combustor is inlet air flow rate, which is used to control experiments. Due to the large size of the duct, we measure the air pressure drop in the combustor as an indicator of the air flow rate. The relationship between the mass flow rate and the pressure drop is shown as Equation (1), which is derived based on the Bernoulli Equation.

$$\dot{m} = A\sqrt{\frac{2P_a\Delta P}{R_g T}} \tag{1}$$

Where $\dot{m}$ is the mass flow rate of the combustor (kg/s); P_a is the inlet air pressure (Pa); ΔP is the air pressure drop of the combustor (Pa), R_g is the specific gas constant of air (J/(kg·K)) and T is the inlet air temperature (K). Accordingly, the selected conditions are pressure drop between inlet and outlet, inlet static temperature and inlet total pressure, shown in Table 5.

Table 5

Selected conditions of experiments

Inlet air temperature (K)	303	303	303	303	303	303
Air pressure drop (Pa)	500	1000	1500	2000	2500	3000
Inlet air pressure (Pa)	101325	101950	102700	103950	104075	104950
Corresponding air flow rate (g/s)	40	60	80	100	110	120

At each inlet condition, the fuel flow rate was increased gradually and the spark plug was switched on for about 5 seconds. The lowest fuel-air ratio and the lowest equivalence ratio were recorded upon successful ignition as lean ignition. When the combustion was stable, the fuel flow rate was reduced slowly to blow-off, and the corresponding fuel-air ratio or equivalence ratio was defined as the lean blow-off.

In this study, a successful ignition occurs if the outlet temperature jumps dramatically within 5 seconds of sparking and keeps growing gradually, whilst the blow-off is defined at the time when the temperature experiences the sharpest drop as shown in Fig. 4.

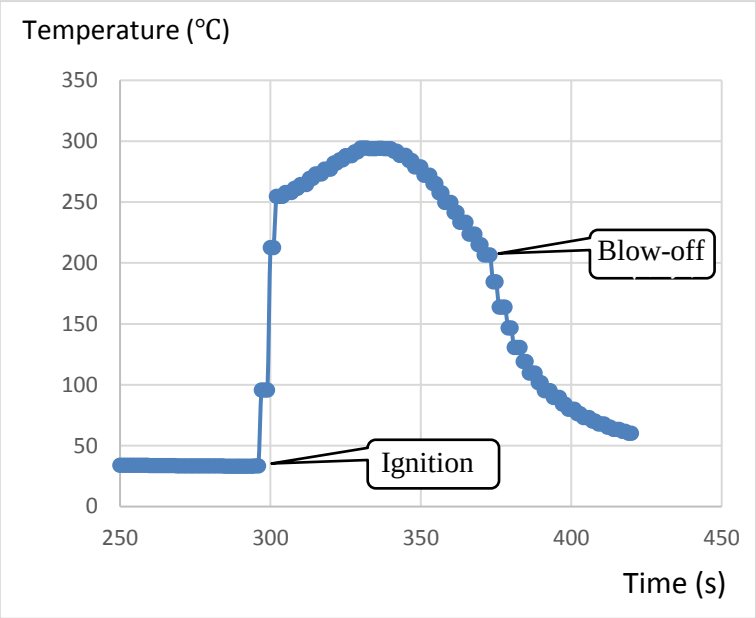

Fig. 4. The definition of lean ignition and lean blow-off

Data processing

Lefebvre proposed two equations on lean ignition and blow-off:

$$q_{LI} = \left[\frac{B}{V_c}\right]\left[\frac{\dot{m}_A}{P_3^{1.5}\exp(T_3/300)}\right]\left[\frac{D_r^2}{\lambda_r H_r}\right] \tag{2}$$

$$q_{LB} = \left[\frac{A}{V_{pz}}\right]\left[\frac{\dot{m}_A}{P_3^{1.3}\exp(T_3/300)}\right]\left[\frac{D_r^2}{\lambda_r H_r}\right] \tag{3}$$

Where q_{LI} and q_{LB} are the fuel/air ratios of lean ignition and blow-off respectively, and $\dot{m}_A$, P_3 and T_3 are the mass flow rate, total air pressure and inlet air temperature. D_r is the mean droplet size of fuel spray, and H_r and λ_r are the lower heating value (LHV) and effective evaporation constant of the fuel. A, B, V_c and V_{pz} are constant geometrical parameters to a certain combustor.

The mas flow rate could be calculated by inlet air pressure and air pressure drop of the combustor. Besides, the inlet air temperature is constant at all operating conditions, and the evaporation constant is associated with air velocity, temperature, pressure, enthalpy of

vaporization and the mean droplet size of fuels. Moreover, the Sauter Mean Diameter (SMD) is a widely used type of mean droplet size and can be calculated by the empirical equation [16]

$$\text{SMD} = \text{constant}\ \sigma^a \mu_f^b m_f^c P_f^d \rho_f^e \tag{4}$$

Where σ and μ_f are the surface tension and dynamic viscosity of the fuel; m_f is the fuel flow rate and P_f is the fuel pressure. For a certain nozzle, the fuel flow rate is determined by the fuel density, fuel pressure and ambient air conditions. The dynamic viscosity of the fuel can be calculated by its kinematic viscosity and density. Therefore, the empirical equation of SMD can be corrected as:

$$\text{SMD} = \text{constant}\ \sigma^a \nu_f^b \rho_f^c P_f^d P_a^e \Delta P^f \tag{5}$$

In order to compare different fuels, the fuel-air ratios of lean ignition and blow-off can be replaced with equivalence ratios, using SMD to represent D_r, and then Equation (2) and (3) can be transferred as follows:

$$\emptyset_{LI} = C_1 \rho_f^a \nu_f^b \sigma_f^c P_{f,I}^d P_a^e \Delta P^f H_{vap}^g H_r^h \tag{6}$$

$$\emptyset_{LB} = C_1 \rho_f^a \nu_f^b \sigma_f^c P_{f,B}^d P_a^e \Delta P^f H_{vap}^g H_r^h \tag{7}$$

Where $\emptyset_{LI}$ and $\emptyset_{LB}$ are the equivalence ratios of lean ignition and blow-off, and ρ_f, ν_f, σ_f, H_{vap} and H_r are the density, kinematic viscosity, surface tension, enthalpy of vaporization and lower heating value of each fuel. The P_a, ΔP, $P_{f,I}$ and $P_{f,B}$, are the inlet air pressure of combustor, the air pressure drop in the combustor, and the fuel pressure when ignition and blow-off happen, whilst C_1, C_2, a, b, c, d, e, f, g and h are constant.

In order to correlate the experimental variables with LI and LB, the Response Surface Methodology (RSM) of DoE was employed. In this study, we selected the Historical-Data of RSM to obtain the equations of lean ignition and lean blow-off. As RSM can only formulate polynomials, Equation (6) and (7) should be linearized by using logarithmic scales as follows:

$$\log_{10}\emptyset_{LI} = C_1 + a\cdot\log_{10}\rho_f + b\cdot\log_{10}\nu_f + c\cdot\log_{10}\sigma_f + d\cdot\log_{10}P_{f,I} + e\cdot\log_{10}P_a + f\cdot\log_{10}\Delta P + g\cdot\log_{10}H_{vap} + h\cdot\log_{10}H_r \quad (8)$$

$$\log_{10}\emptyset_{LB} = C_2 + a\cdot\log_{10}\rho_f + b\cdot\log_{10}\nu_f + c\cdot\log_{10}\sigma_f + d\cdot\log_{10}P_{f,B} + e\cdot\log_{10}P_a + f\cdot\log_{10}\Delta P + g\cdot\log_{10}H_{vap} + h\cdot\log_{10}H_r \quad (9)$$

3. *Results and discussion*

The lean ignition and blow-off

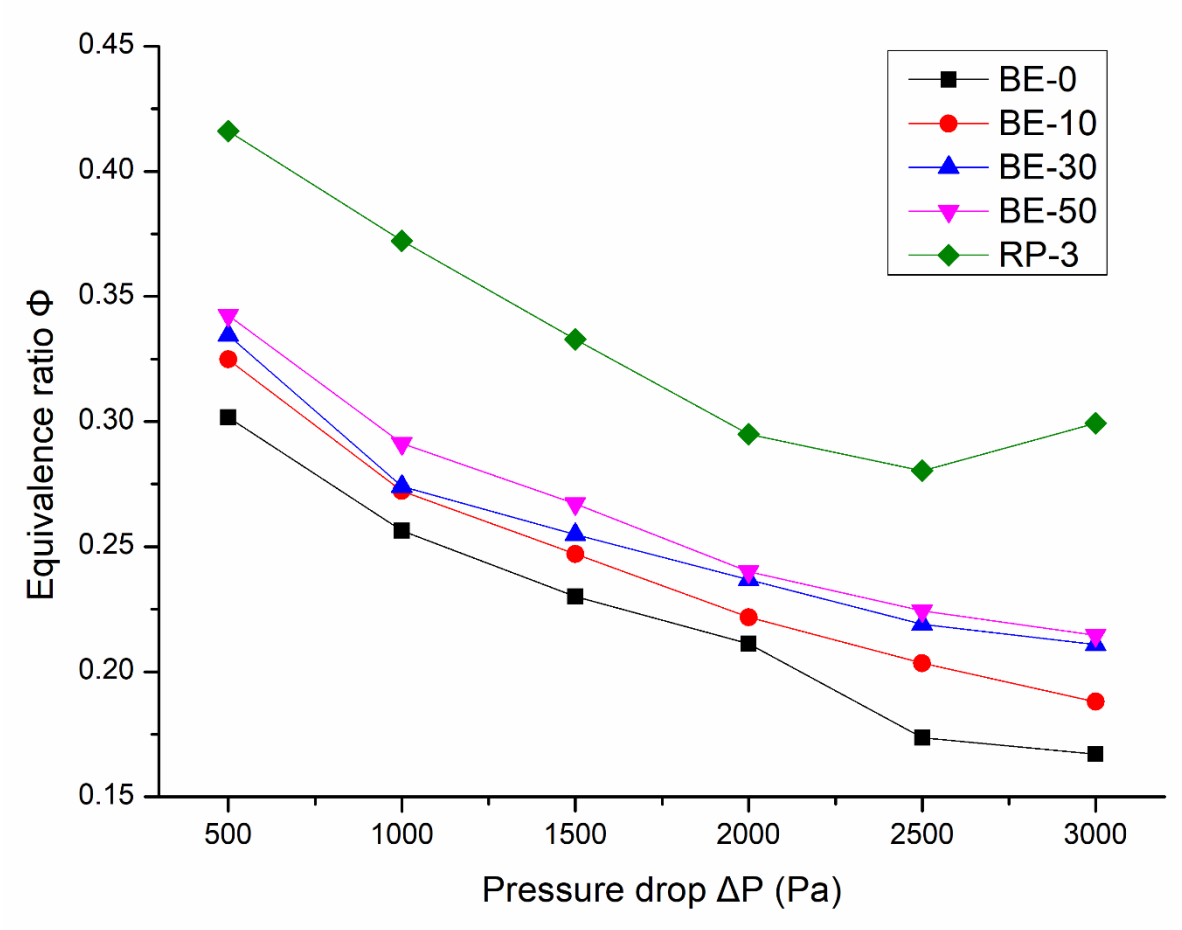

Fig. 5. The equivalence ratio of lean ignition versus the air pressure drop in the combustor

The results of lean ignition tests are shown in Fig. 5. In general, the equivalence ratios of lean ignition ($\emptyset_{LI}$) for all the biofuels drop with the increasing air pressure drop (ΔP) except that RP-3 shows a turning point at the air pressure drop of 2500 Pa. This tendency indicates that lean ignition at lower equivalence ratios was possible when the air flow velocity was high

(with high pressure drop), in other words, all biofuels can be ignited easier compared with RP-3 under lean combustion conditions. The success of ignition is mainly determined by the quality of atomization and the lower heating value (LHV) of fuels. Hence the curves of $\emptyset_{LI}$ versus air pressure drop may be attributable to the fact that high inlet air velocity improves the atomization quality by enhancing droplet breakup and forming well-mixed fuel-air mixture [26].

The turning point of RP-3 indicates that the positive effect of air flow on ignition has reached its maximum, after which the air flow is too high to further facilitate ignition. Fig. 5 illustrates that the equivalence ratios of all the biofuels are approaching to stable values at high air pressure drop. Therefore, it is conceivable that all the biofuels would also have turning points after 3000 Pa.

Fig. 5 also illustrates that all biofuels haver lower equivalence ratios of LI than RP-3 under the same inlet air conditions, which indicates that all biofuels can be ignited easier compared with RP-3. Considering RP-3 has higher LHV than all biofuels, the reason can only be attributed to better spray quality of biofuels, which results in a relatively more homogeneous fuel-air mixture for ignition. Among all the biofuels, pure butyl butyrate has the lowest LI equivalence ratio, and higher ethanol content results in higher LI equivalence ratio for other biofuels. According to the aforementioned analysis, two factors determine the ignition: first, the lower viscosity of fuels promotes atomization process and results in more uniform fuel-air mixtures for ignition; second, fuels of higher LHV release more heat to maintain the stability of initial flames generated by the spark and thus is capable of producing successful ignition. In

this case, the effect of spray quality exceeds that of LHV on ignition when comparing biofuels of lower viscosity with RP-3 of higher viscosity, whilst to all biofuels, LHV is more significant to ignition than spray quality because the LHV of ethanol is significantly lower than others.

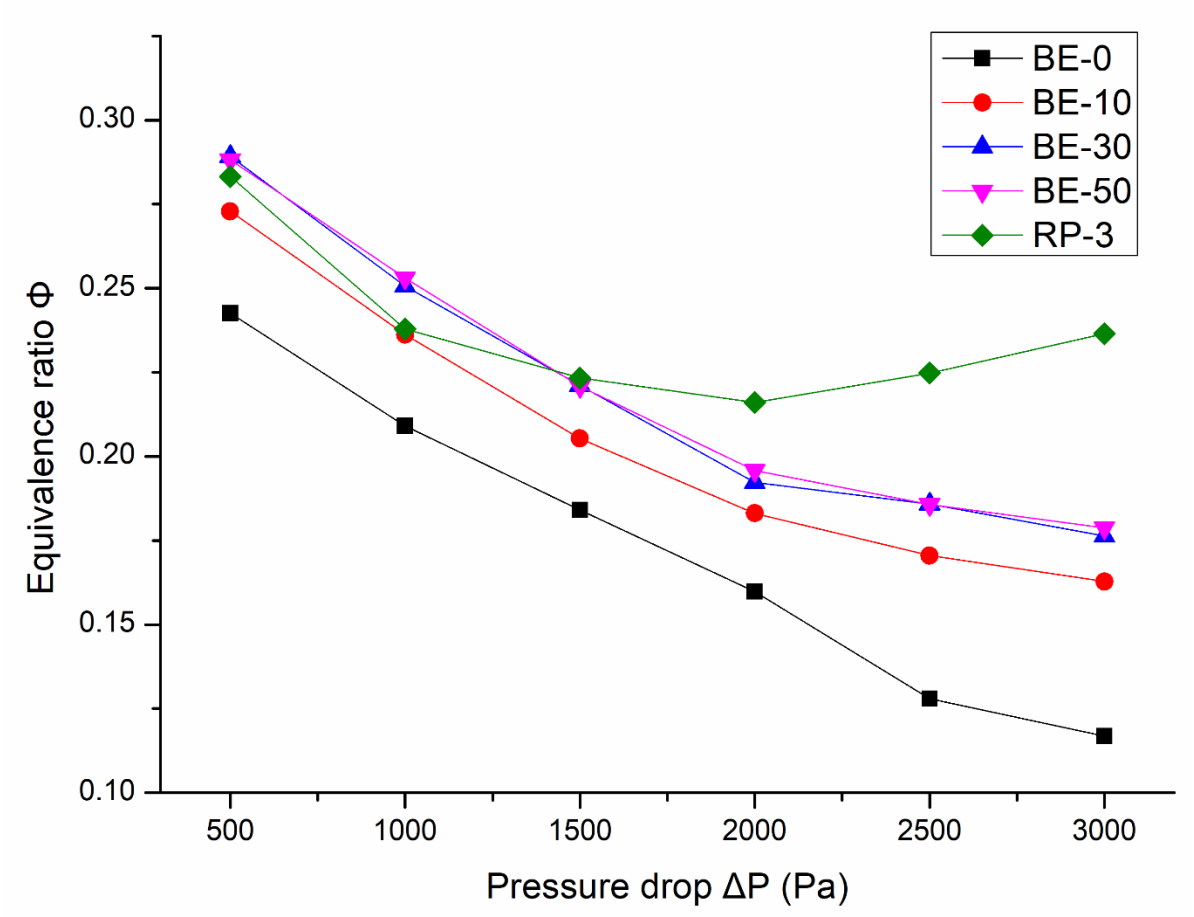

Fig. 6. The equivalence ratio of lean blow-off versus the air pressure drop in the combustor

Similar to LI equivalence ratio, the LB equivalence ratio for most of the biofuels also decreases as the pressure drop increases, but RP-3 experiences a turning point at the pressure drop 2000 Pa. This tendency indicates that the lean blow-off of biofuels occurs at lower equivalence ratio when the air flow rate or velocity is higher, which means the flame would be more difficult to be blown off under this air condition. According to literature [26, 27], high

air flow rate within a certain range can promote spray and thus contributes to stabilizing the flame instead of blowing it off.

The turning point of RP-3 means the positive impact of high air flow on the stability of flame reaches its maximum, after which high air flow tends to blow off the flame. Fig. 6 also shows that the $\emptyset_{LB}$ of all the biofuels become stable at higher pressure drop, which implies that the biofuels would also experience their turning points if the air flow keeps growing. The difference of LI equivalence ratio between RP-3 and biofuels is mainly caused by the comprehensive effects of their spray properties and LHV.

Blow-off is a process which breaks the balance between the heat released by flames and heat absorbed by the air flow. Therefore, fuels with higher LHV produce more heat during combustion, which makes it easier to maintain the stability of flames. Meanwhile, biofuels, especially those with ethanol, have better spray qualities and thus result in more uniform fuel-air mixture facilitating stable combustion. Fig. 6 shows that the $\emptyset_{LB}$ of biofuels decreases with ethanol increasing, whilst the $\emptyset_{LB}$ of RP-3 is lower than that of BE-30 and BE-50 prior to its turning point and then increases to the highest. This trend illustrates that among all the biofuels, the effect of LHV is not as significant as spray quality when the air pressure drop is in the range of 1500 Pa to 3000 Pa. Nevertheless, compared with BE-30 and BE-50, the LHV of RP-3 plays a more important role in anti-blow-off than spray under low air flow condition (air pressure drop less than 1500 Pa), whilst spray becomes more significant under high air flow condition.

The equivalence ratio of lean ignition is higher than that of lean blow-off under the same air conditions. Because once the fuel is ignited at the lean ignition boundary, it keeps

combusting at leaner condition until the equivalence ratio drops to the lean blow-off boundary. It means less fuel can be used to maintain stable combustion after a successful ignition. Therefore, we name the difference between the two boundaries as leanest stable combustion range (LSCR) of the fuel, a factor to estimate how difficult the fuel can keep stable combustion with least fuel consumption. Consequently, the LSCR can also be used to evaluate the stability of combustion of a fuel from a new perspective. . The LSCR of all fuels can be calculated and shown in Fig. 7.

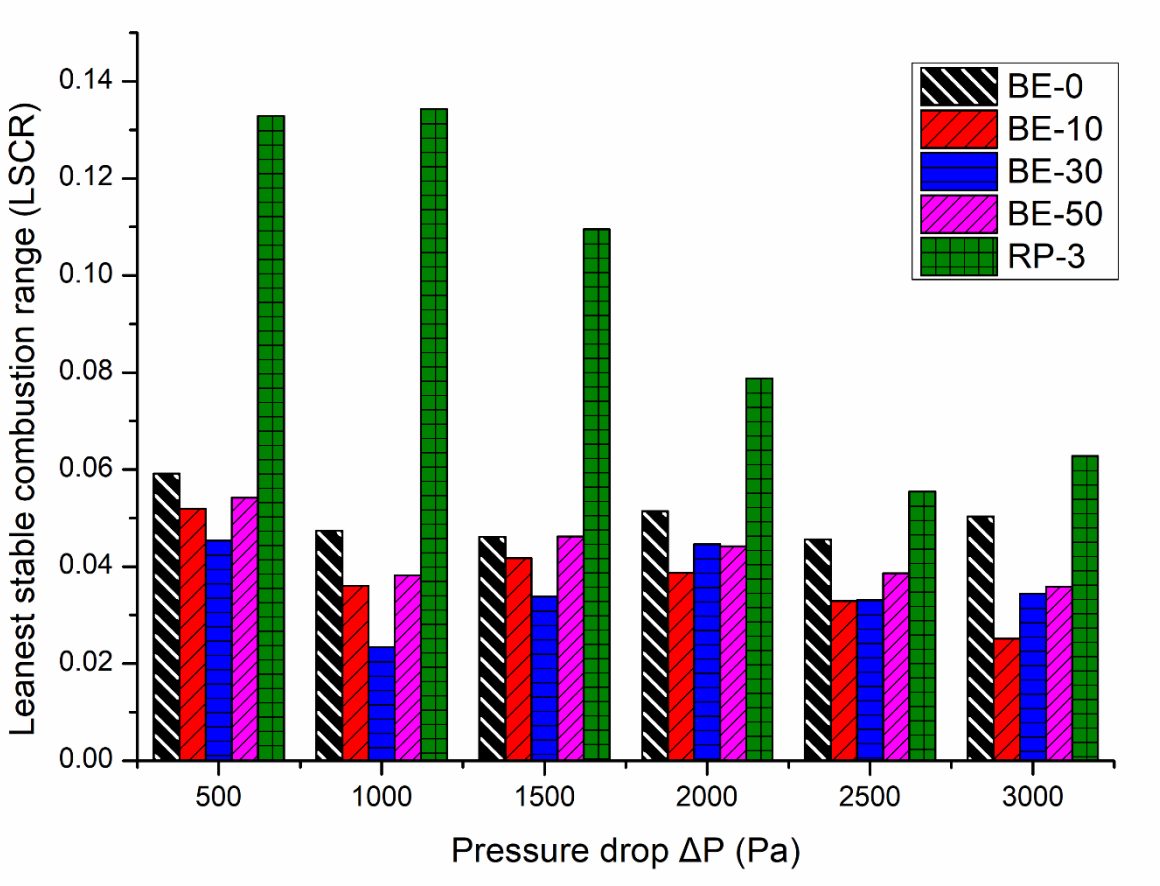

Fig. 7. The leanest stable combustion range (LSCR) of all fuels

The LSCR of RP-3 shows different tendency from those of biofuels. First, the overall LSCR of RP-3 is quite larger and changes more significantly as the air pressure drop increases compared with biofuels. The phenomena indicate that RP-3 can combust stably in a larger

range of equivalence ratios but the stability is sensitive to the change of air flow. In contrast, the leanest stable combustion of biofuels can only be achieved in a small range of equivalence ratios, yet the stability is not susceptible to air flow change. On one hand, RP-3 has significantly higher LHV than biofuels, which enables it to release more heat to maintain stable combustion when it is burning at different air conditions, and thus cause larger LSCR than biofuels. On the other hand, biofuels are easier to atomize than RP-3 and so their sprays have been fully developed at smaller air flow and cannot change significantly when the air flow changes. Consequently, the LSCRs of biofuels only fluctuate slightly compared to that of RP-3. On the other hand, the LSCR of RP-3 is a unimodal curve with one spike at 1000 Pa and one trough at 2500 Pa, whilst the LSCRs of biofuels are bimodal curves with two troughs at 1000 Pa and 2500 Pa. Because RP-3 has lower equivalence ratio of lean blow-off at 1000 Pa air pressure drop than most biofuels and thus enlarges its LSCR. It indicates RP-3 can maintain its combustion more easily with less fuel consumption at 1000 Pa air pressure drop, whilst biofuels are easier to be blown off. In general, RP-3 has significantly higher stability of combustion than biofuels at lower air flow rate especially at 1000 Pa air pressure drop, however, the stability of RP-3 reduced dramatically at high pressure drop, while the combustion stability of biofuels only change slightly at different air flow rates. The biofuel LSCR experiences a U-shaped curve with the ethanol content increasing from 0 to 50%. In other words, the LSCR is high for both BE-0 and BE-50 but it is low for BE-10 and BE-30. Ethanol is found to have two contradictory effects on both LI and LB: lowering the viscosity to promote fuel atomization and reducing the LHV of the fuel to deteriorate combustion quality. It is conceivable that the U shaped curve of the LSCR for biofuels could be the result of the two effects. When ethanol

content increases from zero, the change of viscosity is not as significant as the reduction of LHV, which reduces the LSCR. However, when ethanol content increases to a certain value, the promotion of atomization exceeds the reduction of LHV.

Model formulation

As mentioned above, the polynomial models are formulated by DoE method based on mathematic and statistics to correlate experimental factors (fuel pressure, inlet air pressure, air pressure drop and fuel properties) with responses (the equivalence ratio of lean ignition and blow-off). Meanwhile, the significance of each factor on responses are also analysed via the DoE approach.

Consequently, an analysis of variance (ANOVA) is performed to investigate the fitness and significance of the formulated models and all factors, as shown in Table 4. The factor A, B, C, D and E refer to the LHV (H_r), air pressure drop in the combustor (ΔP), fuel pressure of ignition or blow-off ($P_{f,L}$ or $P_{f,B}$) and the inlet air pressure of the combustor (P_a), whilst the R1 and R2 stand for the equivalence ratio of lean ignition and blow-off.

Table 6

ANOVA of experimental factors and the models

Factors	R1		R2	
	F-value	P-value	F-value	P-value
Model	356.04	0.0001	254.89	0.0001
A	79.72	0.0001	15.4	0.0005
B	62.26	0.0001	45.4	0.0001
C	39.76	0.0001	90.12	0.0001

D	7.84	0.0093	6.81	0.0146
Lack of fit	0.70	0.7509	0.4	0.9505
R2		0.9814		0.9742
Adj R2		0.9786		0.9704
Pred R2		0.9746		0.9631
Adeq Precision		71.339		62.16

The F-value in Table 6 is the test for comparing model variance of a factor with its residual (error) variance. Accordingly, a high F-value (>1) is acceptable because it indicates that the factor has a significant effect on the response. The P-value is the probability of error value. A P-value less than 0.05 indicated that there was a statistically significant difference between the means, but a P-value larger than 0.1 implies no difference between the means. Normally, it is overall significant when the P-value of the model is less than 0.05 and that of each factor is less than 0.1. For example, the factor A for R1 has an F-value of 79.72 and a P-value of 0.0001, which means the factor B has an significant effect on R1 and there is only 0.01% chance that the F-value of 79.72 occurs due to noise. The P-values of ρ_f, ν_f, σ_f, H_{vap} are all larger than 0.1, so they are discarded in the model and not listed in the ANOVA table.

Lack of fit is measuring how poor the model fits the data. A strong lack of fit (F-value>1 or P-value<0.05) means the model cannot fit the data well. For instance, that the lack of fit of R2 has an F-value of 0.4 and a P-value of 0.9505 implies that the model error (residuals excluding replicate variation) is significantly less than the replicate error.

The R^2 is a measure of the amount of variation around the mean explained by the model, and the Adj R^2 is that adjusted to compensate for the addition of variables to the model. As

more independent variables are added to the model, R^2 will increase. In contrast, the Adj R^2 can increase or decrease depending on whether the additional variable adds or detracts to the explanatory power of the model. For this reason, Adj R^2 is considered to be a more accurate indicator than R^2 [19]. Consequently, high R^2 (close to unity) and Adj R^2 are acceptable for the model. The Pred R^2 is used to predict new data by this model. The Adeq Precision is a signal-noise ratio, which compares the range of the predicted values at the design points to the average prediction error. A statistically sound model can be obtained if the difference between the Pred R^2 and Adj R^2 is within 0.2 and high Adeq precision is larger than 4. In this research, the models of R1 and R2 have high R^2, Adj R^2 and Adeq Precision, and the differences between the Pred R^2 and Adj R^2 are quite small. Therefore, the two models show accurate prediction with high signal to noise ratio.

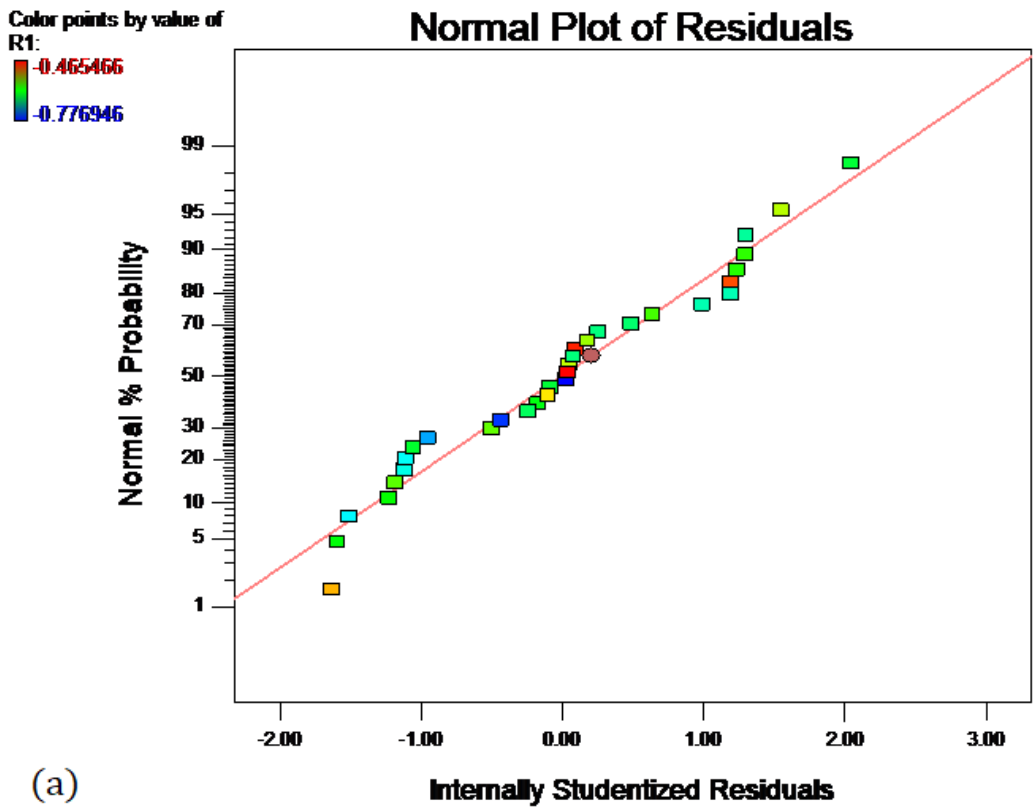

(a)

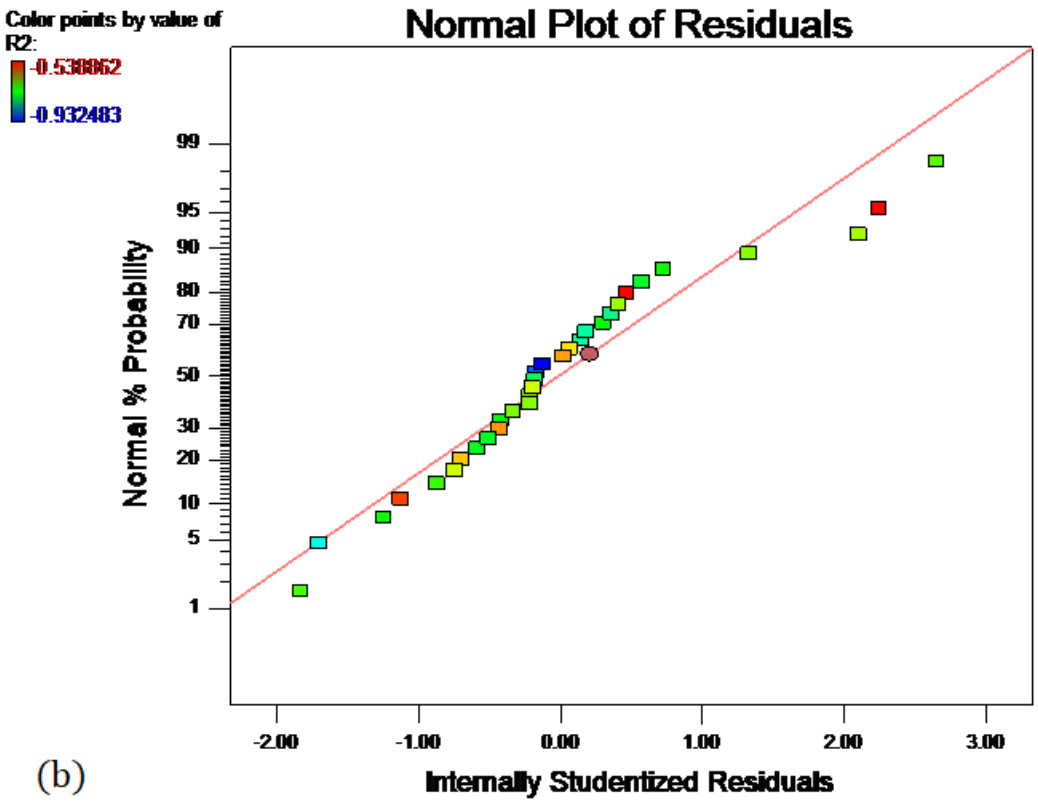

Fig. 8. Normal probability plots of residuals for R1 (a) and R2 (b)

The model error (residuals) consists of normally distributed random variation from the experimental process, which brings in a method to assess the model validity by diagnosing whether the residuals follow a normal distribution. As shown in Fig. 8, the points of experimental data narrowly scatter around the straight lines in the normal probability plots. It indicates that the residuals for R1 and R2 follow normal distributions well and the derived models will not be improved by any transformation to R1 and R2, which means the models are valid.

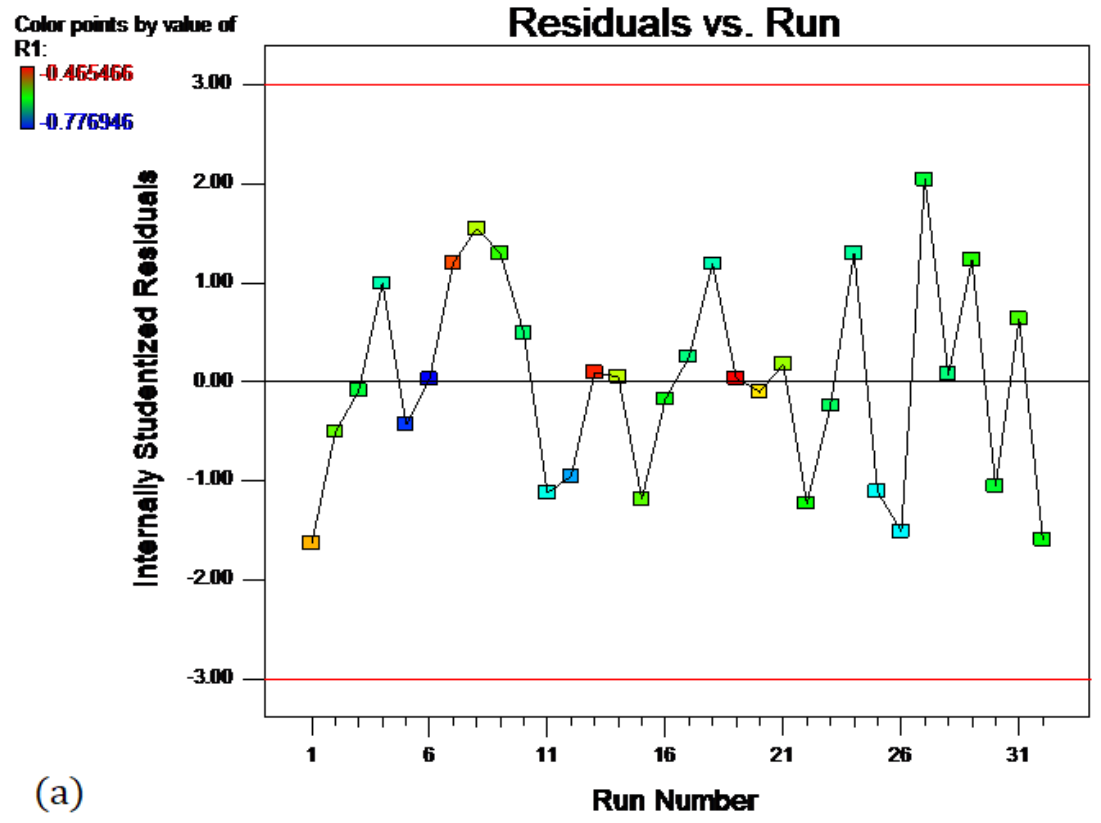

(a)

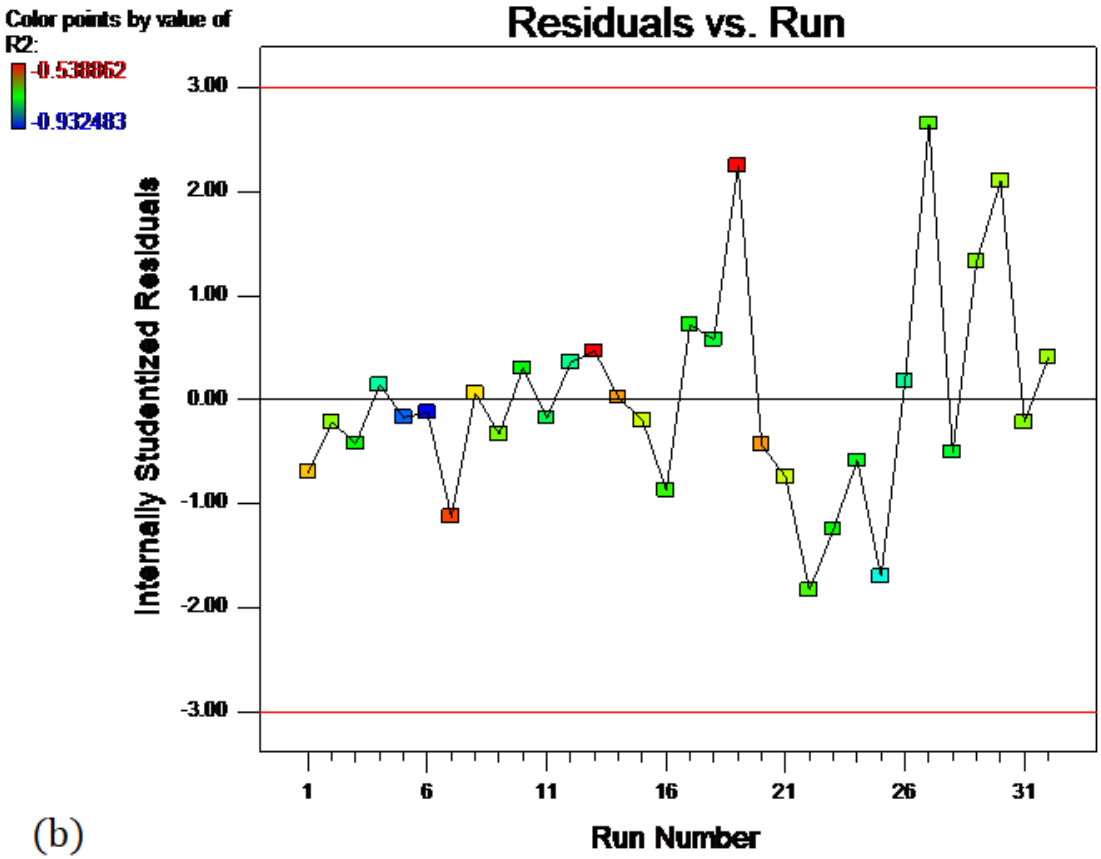

(b)

Fig. 9. Residuals of R1 (a) and R2 (b) vs the run order of experiments

The residuals vs run plots are used to check for lurking time-related variables that may influence the response during experiments. A random scatter means no systematic effect on response is caused by the run order of experiments. In Fig. 9, the residuals of R1 and R2 show no evident trends when plotted versus the run order of experiments, which indicates the possibility can be excluded that R1 and R2 are impacted by any time dependent factors.

Fig. 10 compares the actual (experimental) data and predicted values by the DoE models of R1 and R2, and the points scatter along the line in the middle closely. This confirms that the derived DoE models is precise to predict R1 and R2. The results also agree with Table 6 where the P-value of R1 and R2 are both 0.0001 and the R^2 is 0.9814 and 0.9742 respectively.

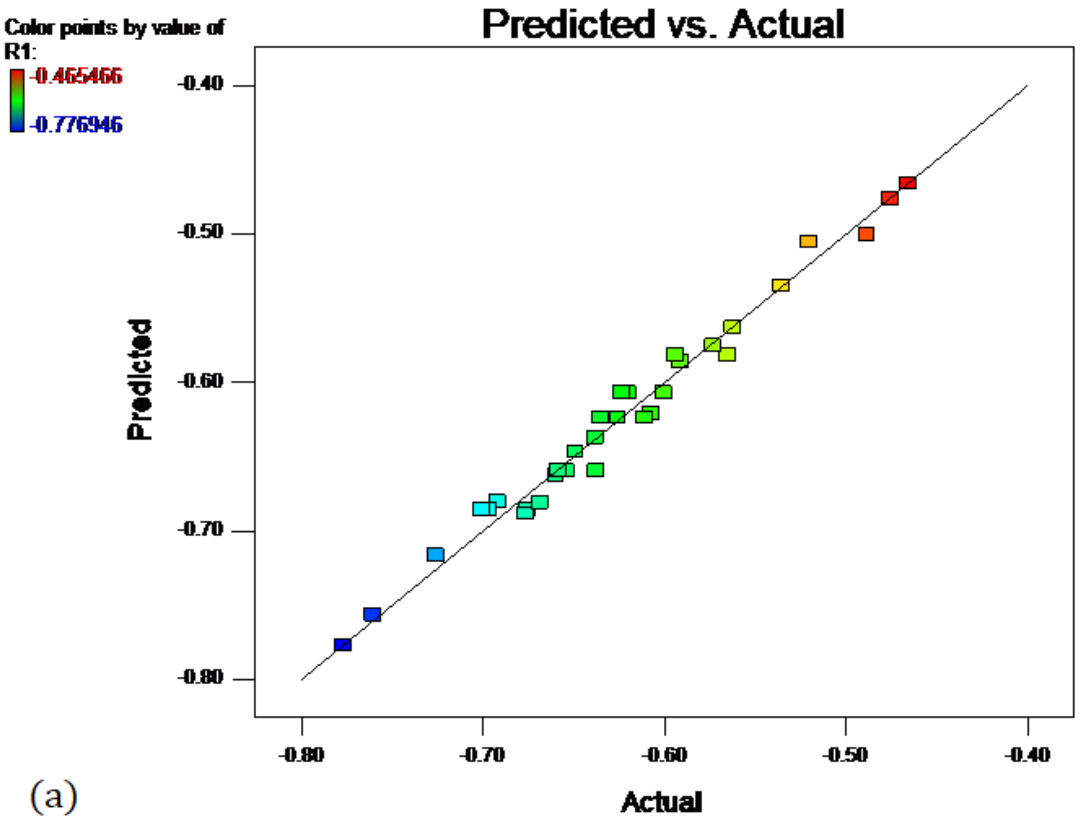

(a)

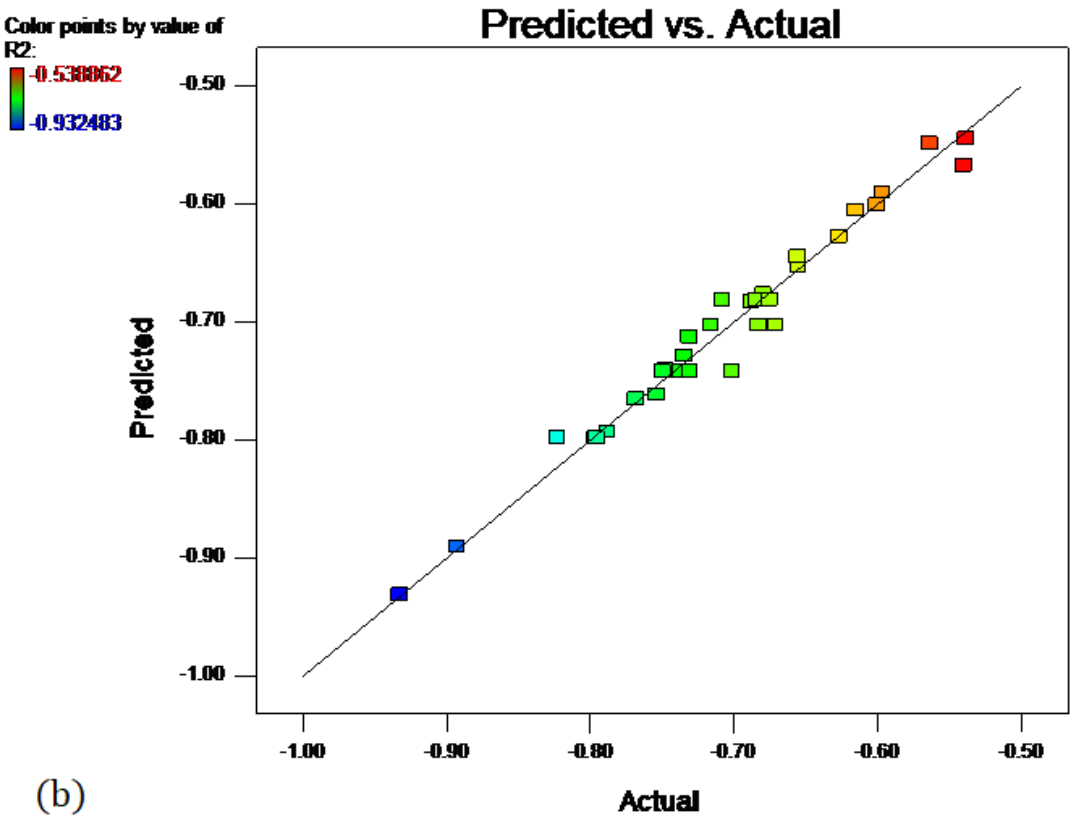

Fig. 10. The predicated values by the models of R1 (a) and R2 (b) vs the experimental data

After the analysis of variance (ANOVA) and the diagnostics, the DoE models of R1 and R2 are then evaluated and verified in the form of Equation (8) and (9). The coded Equation (10) and (11) are firstly obtained to quantitively analyse the effect of each factor on responses regardless of its unit. In the coded equations, the four factors A, B, C and D are coded to the interval of [-1, 1] as shown in Table 7.

Table 7

The coded factors and their levels in the analysis on R1 and R2

Variable	Factor	Unit	R1		R2	
			-1	1	-1	1
$\boldsymbol{H_r}$	A	MJ/kg	-0.032	-0.020	-0.028	-0.00874
$\boldsymbol{\Delta P}$	B	Pa	-0.16	-0.093	-0.18	-0.098
$\boldsymbol{P_f}$	C	Pa	0.027	0.053	0.073	0.11

$\boldsymbol{P_a}$	D	Pa	-0.064	-0.00987	-0.089	-0.011	

$$R_1 = -0.59 - 0.026 \cdot A - 0.13 \cdot B + 0.04 \cdot C - 0.037 \cdot D \quad (10)$$

$$R_2 = -0.67 - 0.018 \cdot A - 0.14 \cdot B + 0.093 \cdot C - 0.05 \cdot D \quad (11)$$

The definition of A, B, C, D, R_1 and R_2 are the same as those in Table 6. The coefficients of the coded models equal to the importance of each factor in Equation (10) and (11): A positive value indicates a synergistic effect, whilst a negative value indicates an antagonistic effect, and the absolute value indicates the significance to the R1 and R2. From the Equation (10) and (11), we can see factor B has the most significant effect on reducing R1 and R2, which agrees with the results in Fig. 5 and Fig. 6 that the equivalence ratio of lean ignition and blow-off decreases fast with increasing air pressure drop, and C has a significantly positive effect on R1 and R2.

The uncoded model shows the actual relationship between the equivalence ratios and experimental variables:

$$\log_{10} \emptyset_{LI} = 29.17 - 0.8591 \cdot \log_{10} H_r - 0.3033 \cdot \log_{10} \Delta P + 0.2179 \cdot \log_{10} P_{f,I} - 5.707 \cdot \log_{10} P_a \quad (12)$$

$$\log_{10} \emptyset_{LB} = 38.21 - 0.6130 \cdot \log_{10} H_r - 0.3384 \cdot \log_{10} \Delta P + \ 0.3334 \cdot \log_{10} P_{f,B} - 7.684 \cdot \log_{10} P_a \quad (13)$$

Where the H_r, ΔP, P_a, $P_{f,I}$ and $P_{f,B}$ refer to the lower heating value (LHV) of test fuel, air pressure drop in the combustor, inlet air pressure of the combustor, fuel pressure of ignition and blow-off, whilst the $\emptyset_{LI}$ and $\emptyset_{LB}$ are the equivalence ratio of lean ignition and blow-off.

Therefore, the final model correlating the equivalence ratio of lean ignition and blow-off with significant experimental variables are shown below:

$$\emptyset_{LI} = 29.17 H_r^{-0.8591} \Delta P^{-0.3033} P_{f,I}^{0.2179} P_a^{-5.707} \quad (14)$$

$$\emptyset_{LB} = 38.21 H_r^{-0.6130} \Delta P^{-0.3384} P_{f,B}^{0.3334} P_a^{-7.684} \quad (15)$$

With this model, the lean ignition and blow-off of butyl butyrate-based biofuels can be predicted precisely. The models indicate that the LHV, air pressure drop in the combustor, inlet air pressure of the combustor all have negative impact on the equivalence ratio of lean ignition and blow-off and the fuel pressure has a positive effect.

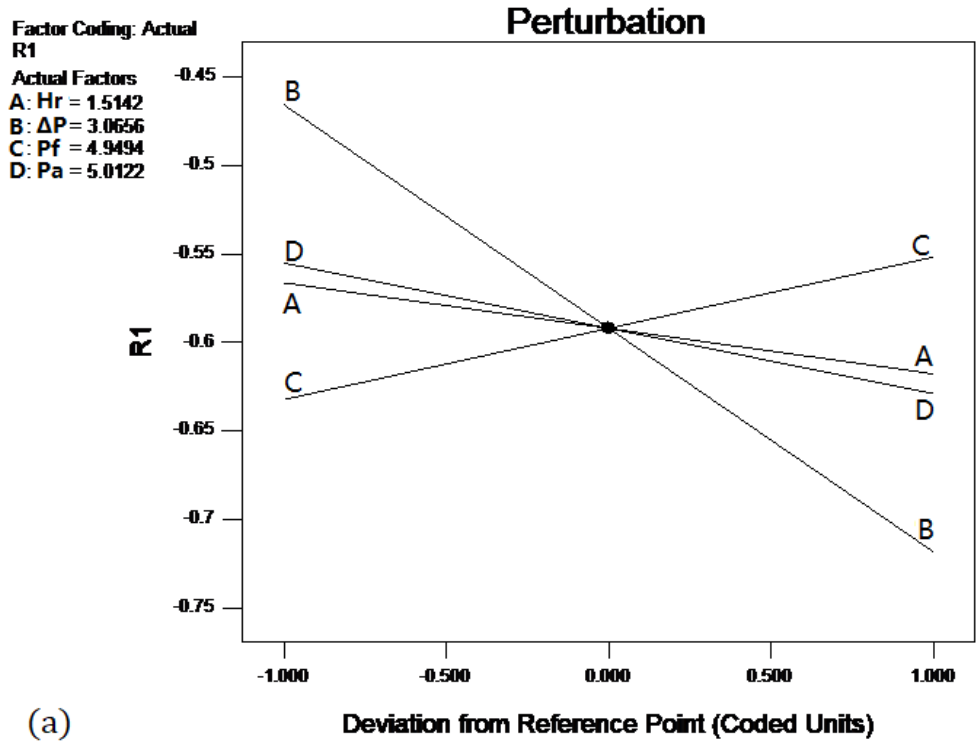

(a)

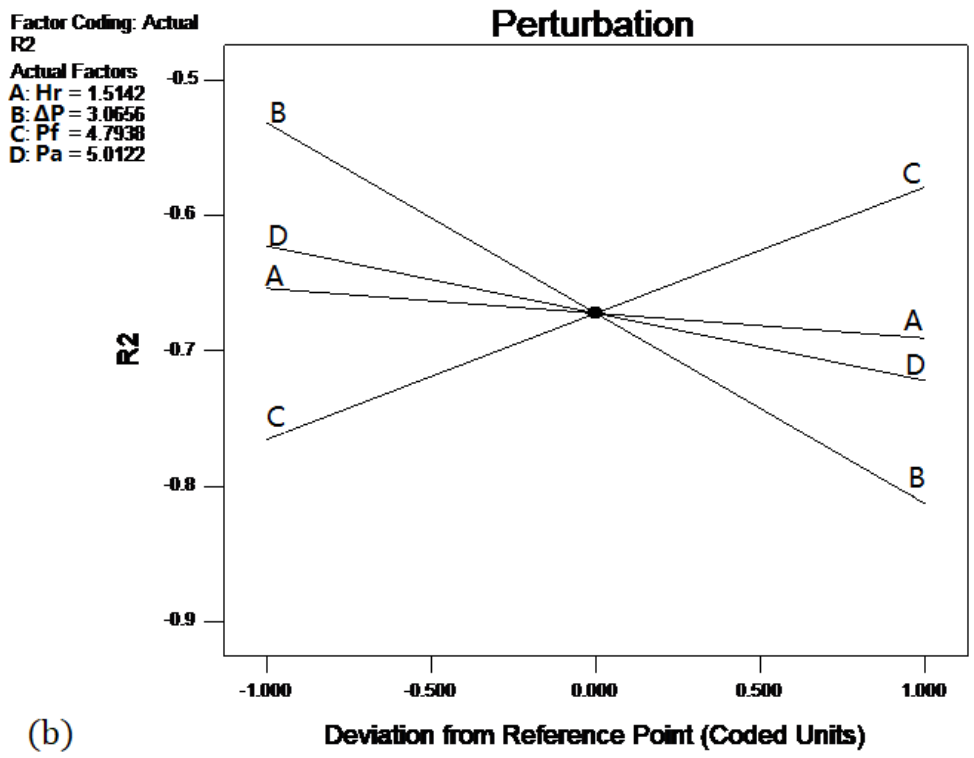

Fig. 11. Perturbation plots of the R1 (a) and R2 (b) models

The perturbation plot is employed to compare the effects of all the factors at a particular point (usually the midpoint) under experimental conditions. In the perturbation plots, the responses are plotted by changing only one factor over its range while holding all the other factors constant. Therefore, a steep slope of a factor shows that the response is sensitive to that factor, whilst a flat line shows insensitivity of the response to it. As shown in Fig. 11, the equivalence ratios of lean ignition and lean blow-off are most sensitive to factor B (ΔP), which is also in consistence with the results in Fig. 5 and Fig. 6, whilst the LHV has most slight effect on lean ignition and blow-off.

4. Conclusions

The paper reports the experimental studies on the Lean Ignition (LI) and Lean Blow-Off (LB) behaviour of butyl butyrate-based biofuels in a gas turbine engine combustor with the air

flow rate ranging from 40 g/s to 120 g/s. The exponential type models of LI and LB were derived via the linear fitting of the DoE approach to quantitatively correlate the equivalence ratios of LI and LB to the LHV, air pressure drop in the combustor, inlet air pressure of the combustor and fuel pressure. The results can be summarised as follows:

1. The equivalence ratios of LI and LB decrease at increasing inlet air flow rate and would experience a turning point at high air flow conditions;
2. All biofuels have lower equivalence ratio of LI than RP-3 mainly due to their better spray quality. Similarly, the equivalence ratios of LB for most biofuels are lower than that of RP-3 except BE-30 and BE-50 at low air flow rates which is because that the influence of LHV surpasses spray quality under certain conditions;
3. The equivalence ratio of LI for all biofuels is lower than that for RP-3 but it grows with increasing ethanol fraction;
4. The overall leanest stable combustion range (LSCR) of RP-3 is larger than that of biofuels but more sensitive to the air condition;
5. The exponential models of LI and LB are obtained, which agree with the experimental data well. Moreover, the obtained equations can also be used to predict the ignition and blow-off behaviour of other fuels;
6. In the models, the LHV, air pressure drop in the combustor, inlet air pressure of the combustor and fuel pressure are all significant factors, among which the air pressure drop in the combustor has the most antagonistic effect and the fuel pressure is the only synergistic one.

The butyl butyrate-based biofuel demonstrated advantages in terms of lean ignition and blow-off characteristics, which makes it a promising fuel candidate for gas turbine engines in aviation application.

Acknowledgement

This research is supported by National Natural Science Foundation of China (91641119). The financial supports from the SAgE doctoral Training Award NH/140671210 and from Chinese Scholarship Council under No. 201508060054 are also acknowledged. The authors also would like to thank the supports from EPSRC through (EP/P001173/1) - Centre for Energy Systems Integration and from Cao Guang Biao High Tech Talent Fund, Zhejiang University.

References

[1] J. Sousa, G. Paniagua, and E. Collado Morata, "Thermodynamic analysis of a gas turbine engine with a rotating detonation combustor," *Applied Energy*, vol. 195, pp. 247-256, 2017/06/01/ 2017.

[2] I. Secretariat, "Annex 16—environmental protection volume II—aircraft engine emissions," ISBN 978-92-9231-123-02008.

[3] M. A. R. do Nascimento and E. C. dos Santos, *Biofuel and Gas Turbine Engines*: INTECH Open Access Publisher, 2011.

[4] T. Seljak, S. R. Oprešnik, M. Kunaver, and T. Katrašnik, "Wood, liquefied in polyhydroxy alcohols as a fuel for gas turbines," *Applied energy*, vol. 99, pp. 40-49, 2012.

[5] Z. Habib, R. Parthasarathy, and S. Gollahalli, "Performance and emission characteristics of biofuel in a small-scale gas turbine engine," *Applied Energy*, vol. 87, pp. 1701-1709, 2010.

[6] J. Sallevelt, J. Gudde, A. K. Pozarlik, and G. Brem, "The impact of spray quality on the combustion of a viscous biofuel in a micro gas turbine," *Applied energy*, vol. 132, pp. 575-585, 2014.

[7] R. W. Jenkins, M. Munro, S. Nash, and C. J. Chuck, "Potential renewable oxygenated biofuels for the aviation and road transport sectors," *Fuel*, vol. 103, pp. 593-599, 2013.

[8] C. J. Chuck and J. Donnelly, "The compatibility of potential bioderived fuels with Jet A-1 aviation kerosene," *Applied Energy*, vol. 118, pp. 83-91, 2014.

[9] L. Chen, Z. Zhang, Y. Lu, C. Zhang, X. Zhang, C. Zhang, *et al.*, "Experimental study of the gaseous and particulate matter emissions from a gas turbine combustor burning butyl butyrate and ethanol blends," *Applied Energy*, vol. 195, pp. 693-701, 2017.

[10] D. W. NAEGELI and L. G. DODGE, "Ignition study in a gas turbine combustor," *Combustion science and technology*, vol. 80, pp. 165-184, 1991.

[11] W. P. Jones and A. Tyliszczak, "Large eddy simulation of spark ignition in a gas turbine combustor," *Flow, turbulence and combustion*, vol. 85, pp. 711-734, 2010.

[12] L. Esclapez, P. C. Ma, E. Mayhew, R. Xu, S. Stouffer, T. Lee, *et al.*, "Fuel effects on lean blow-out in a realistic gas turbine combustor," *Combustion and Flame*, vol. 181, pp. 82-99, 2017.

[13] L. Esclapez, P. Ma, and M. Ihme, "Large-eddy simulation of fuel effect on lean blow-out in gas turbines."

[14] S. Deng, D. Han, and C. K. Law, "Ignition and extinction of strained nonpremixed cool flames at elevated pressures," *Combustion and Flame*, vol. 176, pp. 143-150, 2017.

[15] T. X. Phuoc, C. White, and D. McNeill, "Laser spark ignition of a jet diffusion flame," *Optics and lasers in engineering*, vol. 38, pp. 217-232, 2002.

[16] A. H. Lefebvre, *Gas turbine combustion*: CRC press, 1998.

[17] D.-S. Zhang, W. Liu, Y.-P. Li, and C.-Q. Hu, "Establishment and optimization of an HPTLC method for the analysis of gatifloxacin and related substances by design of experiment," *JPC-Journal of Planar Chromatography-Modern TLC*, vol. 26, pp. 215-225, 2013.

[18] M. A. Jaoudé, J. Randon, C. Bordes, P. Lanteri, and L. Bois, "A design of experiment approach to the sol–gel synthesis of titania monoliths for chromatographic applications," *Analytical and bioanalytical chemistry*, vol. 403, pp. 1145-1155, 2012.

[19] C. T. S. Turk, U. C. Oz, T. M. Serim, and C. Hascicek, "Formulation and optimization of nonionic surfactants emulsified nimesulide-loaded PLGA-based nanoparticles by design of experiments," *AAPS PharmSciTech*, vol. 15, pp. 161-176, 2014.

[20] L. Chen, Z. Zhang, W. Gong, and Z. Liang, "Quantifying the effects of fuel compositions on GDI-derived particle emissions using the optimal mixture design of experiments," *Fuel*, vol. 154, pp. 252-260, 2015.

[21] L. Chen, Z. Liu, P. Sun, and W. Huo, "Formulation of a fuel spray SMD model at atmospheric pressure using Design of Experiments (DoE)," *Fuel*, vol. 153, pp. 355-360, 2015.

[22] P. A. Glaude, R. Fournet, R. Bounaceur, and M. Molière, "Ethanol as an alternative fuel in gas turbines: Combustion and oxidation kinetics," in *ASME Turbo Expo 2010: Power for Land, Sea, and Air*, 2010, pp. 555-562.

[23] A. H. Lefebvre and D. R. Ballal, "Gas Turbine Combustion: Alternative Fuels and Emissions, (2010)," ed: CRC Press.

[24] T. Johansen and J. Schramm, "Low-temperature miscibility of ethanol-gasoline-water blends in flex fuel applications," *Energy Sources, Part A*, vol. 31, pp. 1634-1645, 2009.

[25] L. Chen and R. Stone, "Measurement of enthalpies of vaporization of isooctane and ethanol blends and their effects on PM emissions from a GDI engine," *Energy & Fuels,* vol. 25, pp. 1254-1259, 2011.

[26] C. ZHANG, J.-c. WANG, Q.-q. QIN, P. DU, X. YAO, Y.-z. LIN, *et al.*, "Experimental research on ignition and lean blowout for micro gas turbine ethanol combustor [J]," *Journal of Aerospace Power,* vol. 9, p. 004, 2009.

[27] Y. Yuan, H. Fan, X. Liu, Q. Dong, C. Tan, and B. Guo, "Analysis on lean blowout of swirl cup combustor at atmospheric pressure condition," *Journal of Thermal Science,* vol. 20, pp. 349-354, 2011.